Decadal to millennial-scale periodicities in North Iceland shelf sediments over the last 12 000 cal yr: long-term North Atlantic oceanographic variability and solar forcing

John T. Andrews [a,*], Jorunn Hardadottir [b], Joseph S. Stoner [a], Michael E. Mann [c], Greta B. Kristjansdottir [a], Nalan Koc [d]

[a] INSTAAR and Geological Sciences, P.O. Box 450, University of Colorado, Boulder, CO 80309, USA
[b] National Energy Authority, Grensásvegur 9, 108 Reykjavík, Iceland
[c] Department of Environmental Sciences, University of Virginia, Charlottesville, VA, USA
[d] Norsk Polar Institute, Tromso, Norway

Abstract

Giant piston core MD99-2269 recovered 25 m of sediment in Hunáfloáall, a deep trough on the North Iceland margin fronting the Iceland Sea, and the site of a shelf sediment drift. The rate of sediment accumulation is 2 m/kyr (5 yr/cm); the core terminated in the Vedde tephra ($\sim$12 cal ka). The sediment was sampled at between 5 and 50 yr/sample, including rock magnetic, grain-size, and sediment properties. Data reduction was carried out using principal component analysis. Two PC axes for the 5-yr/sample magnetic data are strongly correlated with measures of coercivity ($ARM_{20\,mT}/ARM$) and magnetic concentrations (kARM). In turn $ARM_{20\,mT}/ARM$ is highly correlated (negatively) with grain-size and the mean size of the sortable silt fraction. Analyses of the two PC axes with MTM spectral methods indicate a series of significant ($>99\%$) periodicities at millennial to multidecadal scales, including those at $\sim$200, 125, and 88 yr which are associated with solar variability. We also document a strong correlation between the sediment magnetic properties and the $\partial^{18}O$ on benthic foraminifera on the North Iceland inner shelf. We hypothesize that the links between variations in grain-size, magnetic concentrations, and solar forcing are controlled by atmospheric and oceanographic changes linked to changes in the relative advection of Atlantic and polar waters along the North Iceland margin. Today these changes are associated with variations in the deep convection in the Greenland and Iceland Seas. The precise linkages are, however, presently elusive although a combination of coarser sediments and low $\partial^{18}O$ values define a Holocene thermal maximum between $\sim$8 and 6 cal ka.
© 2003 Elsevier Science B.V. All rights reserved.

1. Introduction

The oceanography and climatology of the waters on the North Iceland shelf (Fig. 1) have been subject to abrupt change in the last few de-

* Corresponding author. Tel.: +1-303-492-5183;
Fax: +1-303-492-6388.
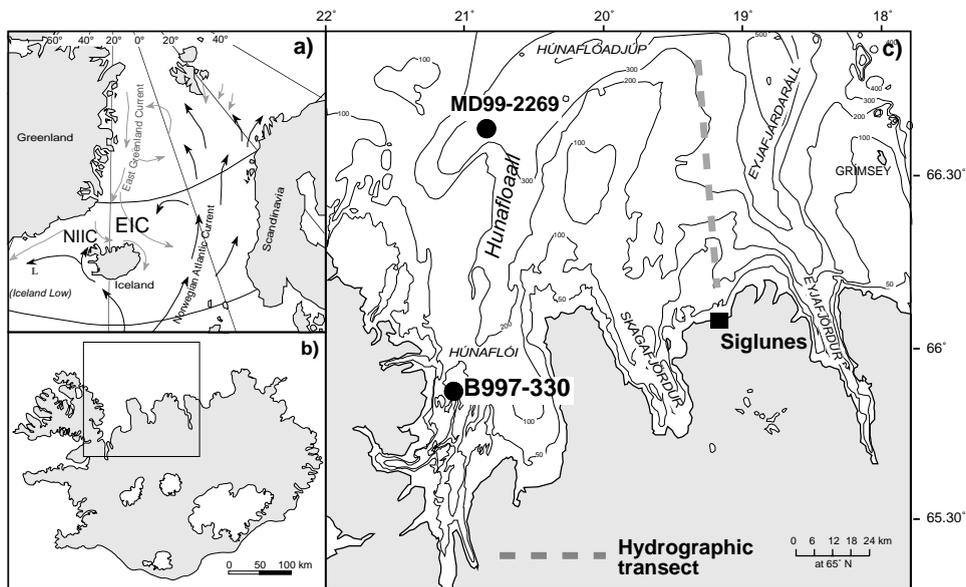 *E-mail address:* andrewsj@colorado.edu (J.T. Andrews).

Fig. 1. Iceland within the North Atlantic (a) and site MD99-2269 off North Iceland (b and c). The Siglunes section is a standard hydrographic transect of the Marine Research Institute (www.hafro.is).

cades [1–4] including a dramatic decrease of 5°C associated with the 1969 Great Salinity Anomaly (GSA). This change was so dramatic that Lamb [5] used the ocean/land interactions associated with this increased advection of Arctic waters as an analog for conditions in the North Atlantic during the Little Ice Age [6]. We present evidence that supports the long-term sensitivity of this area to changes in environmental conditions; we focus on the association between changes in a few simple sediment magnetic parameters on the one hand, and forcings associated with changes in solar activity and the thermohaline circulation (THC), on the other.

As part of the IMAGES V 1999 cruise in the Nordic Seas we obtained core MD99-2269 (henceforth #69) from Húnaflóaáll, a large trough off N/NW Iceland (Fig. 1). The core site had been selected on the basis of a previous cruise in 1997 [7,8]. This area has been surveyed hydrographically for several decades by the Marine Research Institute, Iceland (www.hafro.is). The 1997 July CTD data from cruise B997 [7] exhibited the same basic water mass structure (Fig. 2) seen at nearby sites (e.g. Siglunes transect, Fig. 1) and fully described by Stefansson [9].

Giant piston core MD99-2269 was retrieved from a shelf sediment body (SSB) which forms a unit about 40 km long and ca. 25–30 m thick on the floor of Húnáfloáall(Fig. 2). Landward and seaward the sediment package thins and Holocene sediment thicknesses are between 1 and 6 m. Based on the limited seismic stratigraphy in Húnáfloáall this unit represents, nearly entirely, sediment accumulation during the Holocene [10], hence it is tempting to associate its construction with the development of the North Iceland Irminger Current at the end of the Younger Dryas cold event [11].

At the seafloor, the SSB is bathed by cool Arctic Intermediate Water [9] (Fig. 2). At the sea surface, the site is intermediate in position with respect to the warm and salty Atlantic Water (AtW) carried around NW Iceland in the North Iceland Irminger Current [9,12], and cold, fresh Arctic Water (Fig. 2) being transported south and east in the East Iceland Current. We attribute the construction of the SSB to bottom currents [13,14] however there are no measurements that we have been able to find within Húnáfloáall, although Jónsson [15] has measured long-term
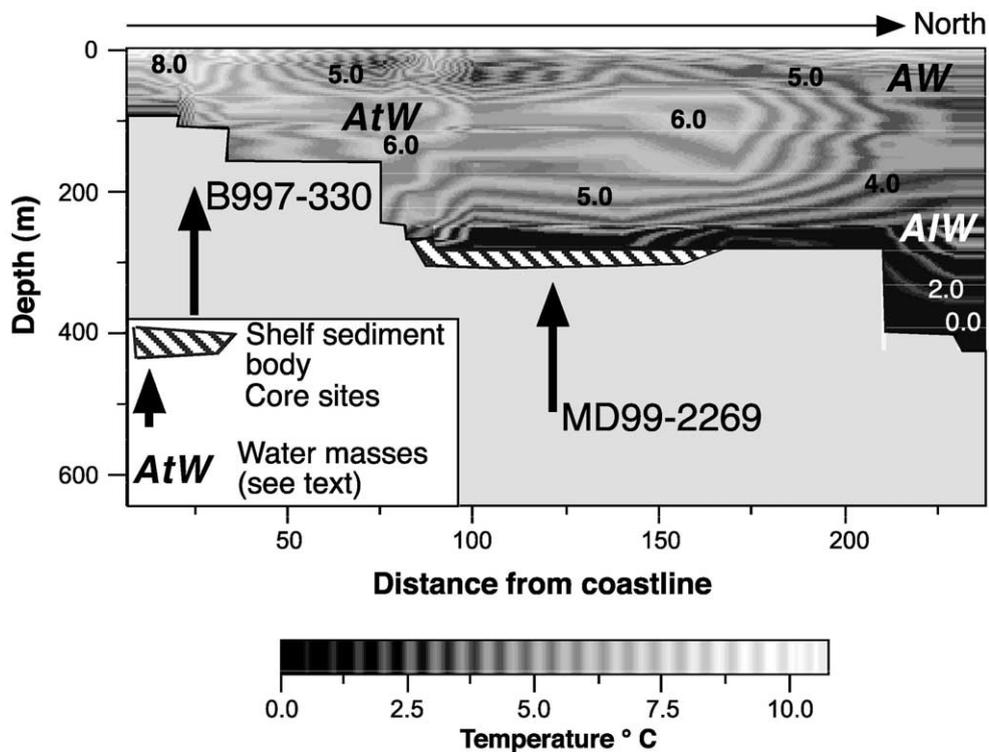
Fig. 2. Potential temperature (°C) and water masses along Hunáflóaall (Fig. 1c), showing the location of the sediment drift body and core sites.

current velocities on the adjoining bank of between 4 and 12 m/s.

2. Materials and methods

The core was measured on board by a GEO-TEKTM MST logger (2 cm) and sediment color determined by a spectrophotometer (5 cm). On shore, archive halves were sampled for continuous rock magnetic measurements using u-channels (rigid u-shaped plastic liners with a square 2-cm cross-section and a length of 1.5 m). Discrete sediment samples were taken at 5-cm intervals from the working-half of the core for carbonate content, mass magnetic susceptibility. Grain-size was measured at 10-cm intervals using a laser-sizing system [16].

The u-channel samples were measured at the Paleomagnetism Laboratory at the University of California-Davis using a 2-G EnterprisesTM model 755 cryogenic magnetometer [17–19] at continuous 1-cm intervals. However, the upper 60 cm ($\sim$285 yr) was not sampled because it was too soft. Smoothing of the measurements occurs over a $\sim$4.5-cm increment associated with the width at the half-height of the response function of the magnetometer pickup coils [17]. Therefore, because each 1.5-m u-channel is measured separately, the ends (top and bottom 4 cm) of each u-channel were omitted from the final data to remove 'edge' effects caused by this smoothing. The data loss ($\sim$5% of the total measured sections) was adjusted by interpolation between end points using AnalySeries [20].

Various measurements and ratios of sediment magnetic properties can be used to describe changes in magnetic concentrations, mineralogy, and grain-size [21–23]. Magnetic concentration is measured both my magnetic susceptibility and by

anhysteretic remnant magnetization (kARM), here we use the latter.

The stability of the ARM to alternating field (AF) demagnetization expressed, for example, as the ratio after 20 mT AF demagnetization to the initial ARM reflects the coercivity spectra of the assemblage which for a magnetite-dominated mineralogy is mostly determined by magnetic grain-size. Initial ARM intensities ranged from 0.4 to > 1.5 A/m. Because of the extremely high concentrations of magnetic minerals, isothermal remanent magnetization (IRM) was so high as to exceed the dynamic range of the instrument in some intervals and these data are not used, but variations in IRM are frequently associated with changes in magnetic mineralogy and the different response of these minerals to different AF demagnetization fields. An initial data set of 10 magnetic variables (see Section 3.1) was employed. Because the sediments primarily represent erosion of the Iceland basalts the sediments can be characterized as having very high concentrations of magnetic minerals and with magnetite (sensus lato) being the dominant mineralogy. The major variations in the sediment magnetic properties are thus related to changes in concentration and grain-size.

We have obtained 11 AMS radiocarbon dates (Fig. 3A). The core is particularly well dated in the last 5 cal ka. These have been calibrated to sidereal years assuming an ocean reservoir correction of ca. 400 yr [24]. Additional age control is provided by the identification of several Hekla tephras that date between 846 (Hekla 1) and 6950 (Hekla 5) cal yr [25]. A prominent seismic reflector occurs at ca. 21 m below sealevel in the SSB. In #69 this reflector has been identified as basaltic ash, with an age and geochemistry equivalent to the Saksunarvatn tephra [26,27]. This eruption has an estimated age in the Greenland ice cores of 10.18 ± 0.06 cal ka [28] and a radiocarbon age of 9 ka [29,30]. The date on the surface sample is contaminated by bomb carbon indicating that we have retrieved sediment ≤ 40 yr old. The dates, including the age for the Saksunarvatn tephra, fit a straight line with the expression: age (cal yr BP) $= -22.8 \pm 92 + 4.9 \pm 0.07 \times$ depth(cm) ($r = 0.998$), with the $\pm$ terms being the one-sigma standard errors on the coefficients.

We used this age/depth model to convert our sediment variables to time series. Because there is no significant change in the rate of accumulation then our time series are indeed equally spaced, which is an important advantage when analyzing the data [31]. The rate of sediment accumulation is sufficiently high that we expect no significant attenuation of multidecadal events [32]. The full sediment data set has been submitted elsewhere [33].

3. Results

3.1. Analysis of sediment magnetic data

Principal component analysis (PCA or EOF analysis) [34] was used to simplify the 10 sediment magnetic parameters and to extract the major orthogonal signals. The 10 parameters measured included: kARM, a succession of ARM AF determinations as a ratio of the original ARM value, NRM J(0)/NRM J(60), IRM J(0)−IRM J(20), and two backfield IRM measurements [22,23]. The first two PCA axes explain 44% and 35% of the variability. Axis 1 is strongly associated with the ratio $ARM_{20 mT}/ARM$ [35], whereas the second axis is highly loaded with kARM (Fig. 3A), a measure of magnetic concentration [21,22]. The stability of a magnetic assemblage to AF demagnetization is a function of mineralogy and grain-size. The AF demagnetization behavior of a sample essentially reflects the coercivity spectra of the assemblage which for a magnetite-dominated mineralogy is mostly determined by magnetic grain-size.

Indeed there is a very strong correlation between $ARM_{20 mT}/ARM$ and grain-size (phi-units) of the sediment (Fig. 3B) with a synthetic correlation [20] of $r = 0.54$. The association between PC1 and the mean size of the sortable silt fraction [36–38] (not shown) is $r = -0.6$. The ratio derived from the intensity of a sample after 20 mT AF demagnetization that had previously been given an ARM normalized by its initial intensity, though only representing a single point on the demagnetization spectra, provides an estimate of the ease (soft) or difficulty (hard) to demagnetize
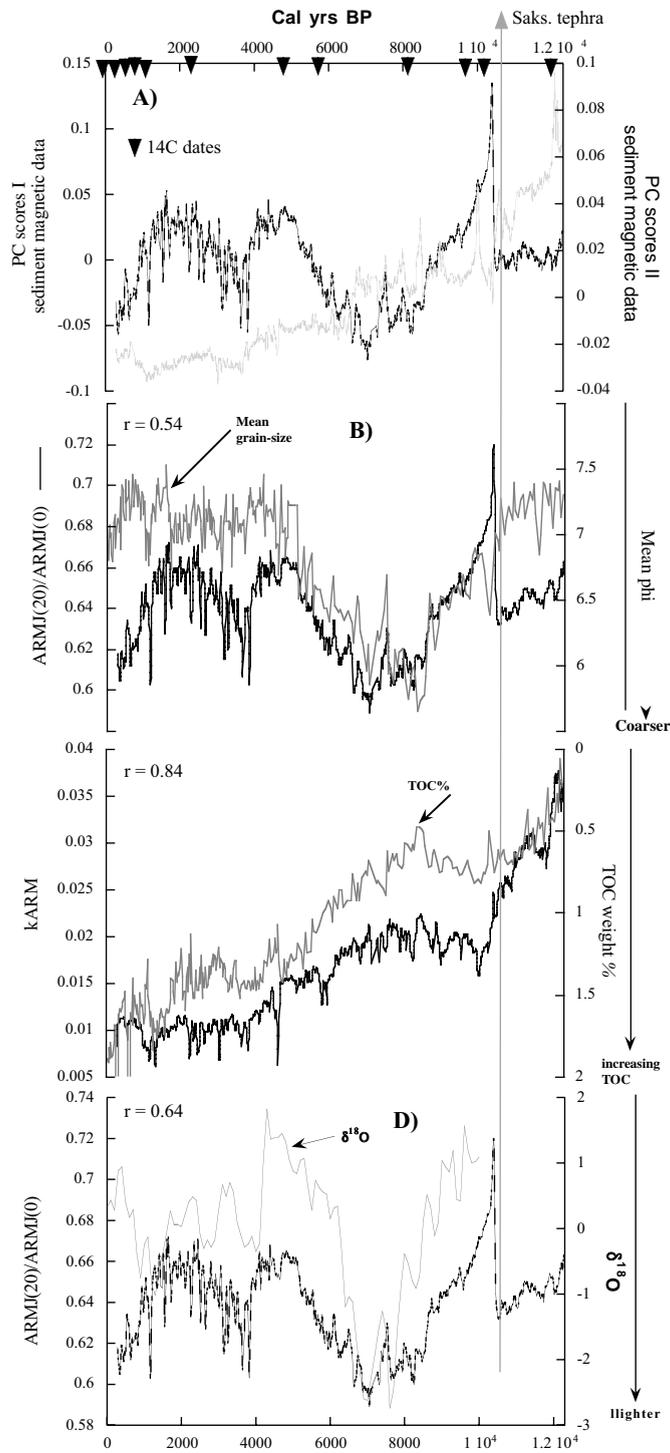
Fig. 3. (A) Time series of sediment magnetic properties represented by the first two principal components which explain 45% and 33% of the variance. The arrow-heads show the location of the radiocarbon dates. (B) Plot of $ARM_{20\,mT}/ARM$ and its correlation with average grain-size (phi-units). (C) Plot of kARM versus TOC wt%. (D) Plot of $ARM_{20\,mT}/ARM$ from MD99-2269 versus the stable isotope data from epifaunal foraminifera in B997-330 (Fig. 1).
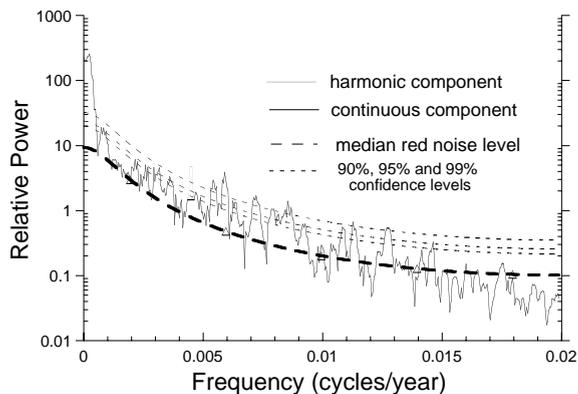
Fig. 4. Spectrum of PC1 as defined in the text. Red noise background and significance levels are determined using the method of Mann and Lees [51], employing a multiple-taper spectral analysis with three tapers and time–frequency bandwidth product 2N. Best-fit red noise background, and 90%, 95%, and 99% significance levels relative to the null hypothesis of a first-order autoregressive 'red noise' process are shown.

a down core sediment sequence. Higher values, therefore, reflect a coarser magnetite assemblage and lower values a finer assemblage. The large peak at 10.2 cal ka (Fig. 3A) is associated with deposition of the Saksunarvatn tephra and represents a prominent 'non-climatic' sediment event. The mean size of the sortable silt fraction lies within the range of analyses from the sediment drifts south of Iceland [36,37], although the magnetic grain-size based on the demagnetization behavior of the ARM suggests that the #69 data are significantly coarser (at least magnetically).

The second principal component, PC2 ($\sim$kARM), is inversely correlated with the total carbonate content of the sediment ($r = -0.81$) and total organic carbon (TOC) ($r = -0.84$) (Fig. 3C) which suggests a dilution of the magnetic signal with these diamagnetic minerals. However, the increase in density with depth from ~ 0.4 g/cc to 0.9 g/cc is not a major control on kARM as the discrete mass magnetic susceptibility measurements (not shown) have an extremely strong correlation with the volume kARM ($r = 0.95$). Mass magnetic susceptibility measurements eliminate the influence of changes in density [22] but it is highly correlated with kARM.

PC scores were calculated from the first two PC

axes and are evaluated in the following section. We have argued [39,40] that total carbonate is an index of marine productivity in these waters [41,42]. At present, high productivity is associated with the presence of AtW on the North Iceland shelf, whereas incursions of cold Arctic/polar waters (such as during the GSA of 1969 AD [4]) resulted in a stratified water column, a marked reduction of nutrients, and a decrease in production in the photic zone [41]. Correlations between changes in carbonate content and the calculated temperatures at Summit, Greenland, are quite striking ($r = 0.71$) [40]. We are still developing our isotope records from #69 [43], but there is a striking similarity between the $\delta^{18}O$ record on the epifaunal species *Cassidulina lobotalus* from B997-330 on the inner North Iceland shelf [44] (Fig. 2) and the $ARM_{20 mT}/ARM$ data from #69 (Fig. 3D). The correlation between the records is high, $r = 0.64$, with sampling resolutions at 5 and 100 yr. The B997-330 $\delta^{18}O$ data match other records from the inner shelf [45,46].

3.2. Frequency-domain behavior

There is increased interest in the behavior of the climate system at different frequencies [47]. In the last decade, attention has focused on millennial-scale periodicities [38,48,49], although varved and other records are now allowing for decadal to century evaluation of marine records [50]. It is within this latter context that we evaluate our data.

Previous work on lower resolution records (50–100 yr/sample), on the North Iceland shelf covering the last 5 cal ka [40], suggested that the carbonate time series hinted at recurring periodicities. In our #69 magnetic data we have substantially higher resolution (each magnetic measurement integrates 20–25 yr (4–5 cm)) making this one of the highest resolution Holocene records available from a marine site in the northern North Atlantic. We compute spectra based on the widely used method of Mann and Lees [51]. This method employs a standard multiple-taper spectral analysis to separate continuous and harmonic components of the spectrum, but measures the significance of these components based on a
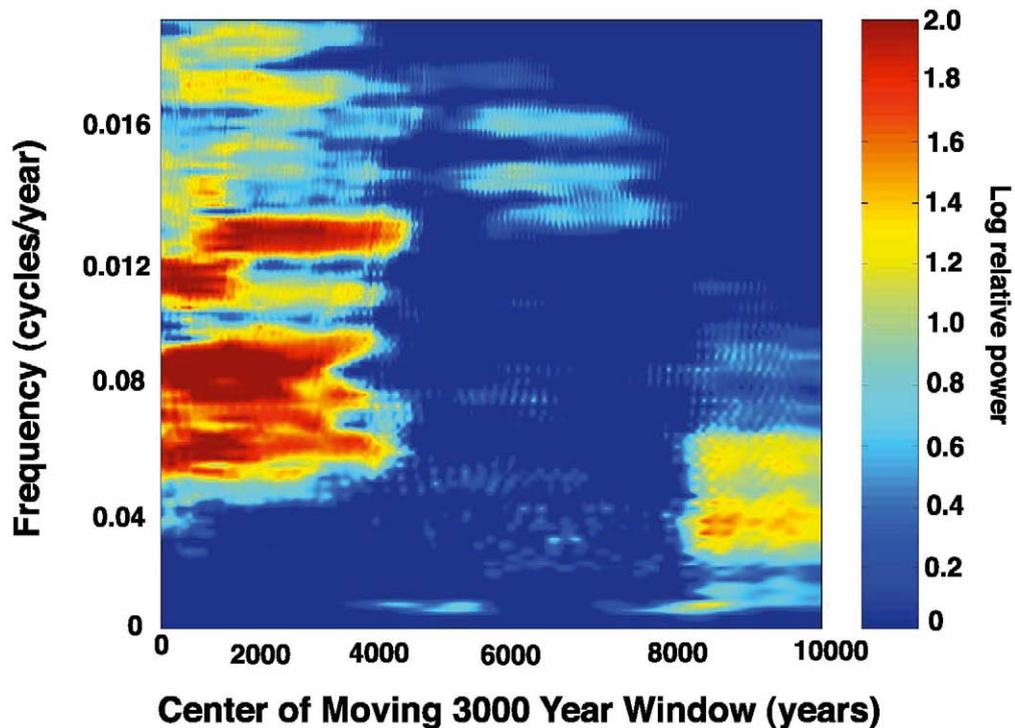
Fig. 5. Evolutive spectrum of PC1 based on a 3000-year moving window, employing the same methodology as in Fig. 4. Time axis corresponds to the center of the 3000-year moving window. The spectrum is shown as the log of the ratio of the spectrum to the estimated red noise background. Only spectral features greater than the mean red noise level (i.e. positive values of the log ratio) are shown, with significance directly proportional to the color scale shown [66].

robust estimate of the red noise background in the time series. The robust noise background is estimated by an analytical fit of the theoretical spectrum for a first-order autoregressive process to a median smooth of the raw spectrum of the time series, using the rules specified by Mann and Lees [51] for selecting the optimal width of the median smoothing window. The spectral analysis is restricted to frequencies $f < 0.02$ cycle/yr (time-scales longer than 50 years), since a break in the red noise background (indicative of a significant loss of recorded variance) is evident at higher frequencies and is probably associated with the above mentioned (see Section 2) integration of the records.

We first computed the spectrum of the cores on the first principal component, which we interpret as a measure of changes in the bottom current velocity along or across the SSB (we have insufficient seismic coverage to reconstruct the sediment architecture of this unit). Nine spectral peaks are found to be significant above the 99% confidence level relative to the null hypothesis of red noise (Fig. 4). Five other peaks are significant above the 95% confidence level. Using three tapers with a time–frequency bandwidth product of 2N, the spectrum can be independently estimated at only 110 frequencies over the interval of interest. Thus, only about one peak on average should exceed the 99% confidence level by chance alone, and the majority of 99% significant spectral peaks are thus likely to be indicative of real features of the spectrum that are inconsistent with a red noise null hypothesis.

The lowest-frequency peak, centered at a $f = 0.0015$–0.002 cycle/yr, corresponds to a significant secular variation, reminiscent of a 5000–6000-year timescale oscillation, that is apparent by visual inspection of the PC1 time series. It is associated with high PC1 scores (Fig. 3A) during the late to
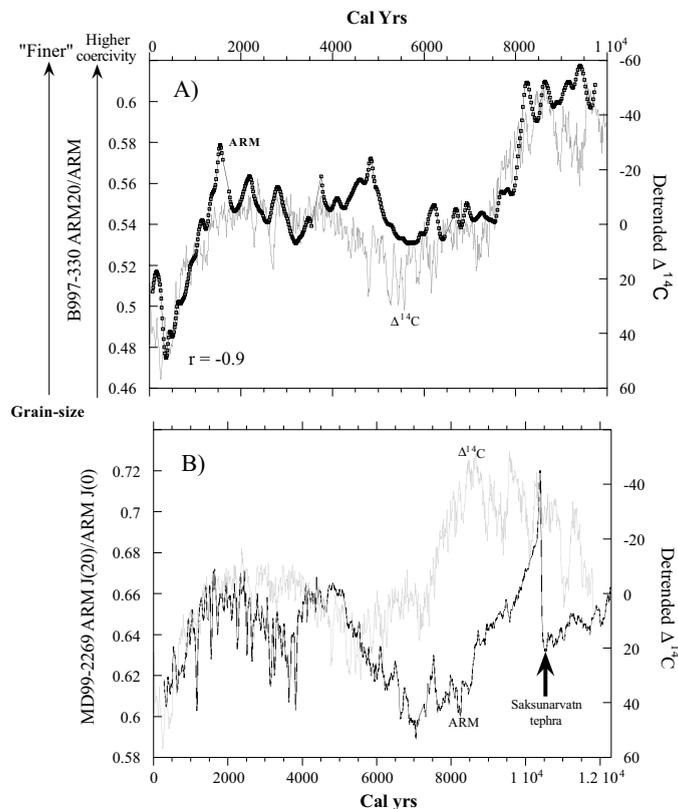
Fig. 6. Correlations between the $ARM_{20\,mT}/ARM$ records from B997-330 (A) and MD99-2269 (B) and the detrended D14C record [24,52].

mid Holocene, low values during the mid to late Holocene, and return to high values again at the end of the Holocene. This long-term secular variation is highly correlated with detrended $\Delta^{14}C$ variations [24,52] (Fig. 6).

A cyclicity close to a 200-year period is also found to be significant at above the 99% level (note: the split peaks at 217 yr and 185 yr are equivalent to a 200-yr period oscillation that is amplitude-modulated at a lower frequency of $f = 0.0008$; interestingly, a peak at $f = 0.0008$ (1250-year period), while not significant at the 99% level, is significant at roughly the 95% level. This signal is consistent in timescale with the 'Suess' wiggles in $\Delta^{14}C$ that have been detected at a period of 208 yr in previous analyses of the $\Delta^{14}C$ data [53]).

In addition, there is a broad range of significant peaks at centennial (170 yr, 140 yr, 125 yr, 118 yr)

and multidecadal (88 yr and 78 yr) timescales (Fig. 4). The 125-yr peak has also been associated with a harmonic of solar periodicities [54], whereas the 88-yr peak corresponds to the well established 'Gleissberg' cycle, the primary component of solar variability associated with the 'Maunder Minimum' period of low sunspot activity during the 17th century. The associated lowering of solar irradiance during this latter period has been related to cold temperatures in Europe through the dynamical influences of a lowering of solar irradiance, which led to the predominance of the North Atlantic Oscillation (NAO) pattern of atmospheric circulation [55]. Interestingly, solar forcing at the 90-yr and ~ 200-yr timescales has also been detected in dust measurements from the GISP2 central Greenland Ice core [56], and variations in the strength of the circumpolar vortex (in essence, variations in the NAO) have been

implicated in explaining past variations in dust concentrations in the GISP2 core [57]. These comparisons indicate a probable link between atmospheric forcing and oceanographic variability on the North Iceland shelf.

We speculate that the broader range of multidecadal and century-scale peaks evident in the PC1 record (Fig. 4) is consistent with the interaction between an intrinsic multidecadal mode of variability in the North Atlantic [58] and a more narrowband external solar forcing at timescales of 88 and 125 yr. Such interactions could be oceanic in nature [59] or mediated through the response of the extratropical atmospheric circulation to solar forcing [55], with a consequent atmospheric-forced response of the meridional overturning of the North Atlantic ocean [60]. Intrinsic coupled ocean-atmosphere dynamics acting on multidecadal timescales appear to give rise to a pattern reminiscent of the 'GSA' [61], with its implied enhanced transport through the Iceland shelf region, shortly following a previous more 'NAO'-like initial atmospheric state. This provides a possible linkage between an initial NAO atmospheric forcing, and the inferred resulting transport variations in the Irminger Current.

To examine possible changes in the nature of preferred periodicities over time, we employed an evolutive spectrum in a 3000-year moving window through the time series. The evolutive spectrum (Fig. 5) shows much of the multidecadal variability (in a frequency range of 0.0125–0.017, periods of 60–80 year) to be persistent through the early Holocene, whereas the century-scale variability (aside from a faint but persistent streak of variance close to the ∼200-year period discussed above) is strong only during late Holocene. It is possible that the low-frequency 5000–6000-year timescale variations modulate the amplitude of higher-frequency variability. This modulation could arise from the non-linear nature of the response of convective overturning to surface forcing. A decrease in the amplitude of century-scale variability between 4000 and 5000 years BP is correlated with a tendency towards weaker inferred shelf transport at that time. This latter tendency, in turn, appears to have been associated with colder temperatures in Europe [38], which

suggests the predominance of the negative phase of the NAO. Due to the positive relationship between the NAO and surface oceanic heat flux over the sub-polar North Atlantic (e.g. [60]), a decreased incidence of winter convective overturning is expected during the negative phase of the NAO although. Such a tendency for decreased convective overturning might also lead to a decrease in variability in convective overturning (since convective overturning cannot be reduced below the 'no convection' level). Such a mechanism would be consistent, for example, with the lesser amplitude century-scale variability in the mid Holocene, though it does not provide a satisfactory explanation for the long-term modulation in the amplitude of multidecadal variability. It is likely that long-term astronomical forcing over the course of the Holocene also plays a role in this regard.

We also computed the spectrum for PC2 which, because of its association with carbonate and TOC content, is interpreted as a signal of marine productivity with variations associated with the interplay between Atlantic and Arctic/polar water mass incursion events, such as those associated with the GSA. The spectrum is dominated by a peak at zero frequency (corresponding to the prominent trend observed in Fig. 3B), but significant variability at the multidecadal to century timescales is also observed. Significant peaks are found in frequency bands centered at roughly 50–60-yr, 70–80-yr, and 100–120-year periods, both in a spectral analysis of the entire record (not shown), and consistently throughout the record in an evolutive spectral analysis employing a 3000-year moving window. It is reasonable to interpret these signals as the signature, in water mass properties, of the same processes influencing current strength discussed earlier.

To investigate possible links between our sedimentary archives and a measure of the THC activity, we examined the 'goodness of fit' between our magnetic grain-size proxy ($ARM_{20\ mT}/ARM$) at sites on the inner and mid North Iceland shelf, and the detrended $\Delta^{14}C$ series [24,52]. The correlation at the inner shelf site (B997-330, Fig. 1), directly influenced by the North Iceland Irminger Current, is a remarkable $r = -0.9$, suggestive of a

very close coupling between these two proxies (Fig. 6A). At site MD99-2269 (Fig. 6B) the agreement is substantial for the last 6 cal ka but is weak for the previous interval. How far this represents an 'interruption' in source/transport/depositional processes caused by the massive Saksunarvatn tephra fallout [27,62] is unclear.

4. Conclusions

In examining the structure of the PC1 scores associated with $ARM_{20\,mT}/ARM$ (Fig. 3) it is our contention that these changes reflect variations in the grain-size and/or supply of sediments associated with the accumulation of the SSB (Fig. 2). The results of our analysis need to be interpreted in the light of the basic threefold oceanographic conditions on the North Iceland shelf (Fig. 2) and how these different water masses would have responded to different forcings, which in turn led to the changes in sedimentary parameters (Fig. 3). The first two principal components of the various sediment parameters largely reflect changes in mineralogy and grain-size (Fig. 3B), and measures of net marine productivity (Fig. 3C). We interpret PC1 as indicative of systematic variations in current transport across the surface of the SSB (Fig. 2).

Present-day observations on the wind stress curl in the Greenland and Iceland Seas and its relationship to deep convection and the thickness of the freshwater layer [63] indicate that low values are associated with a reduction or cessation in convection and an increase in the freshwater layer. We thus hypothesize that intervals of finer grain-size (Fig. 3B) are proxies for a decrease in the wind stress curl, therefore the interval of coarse sediment and low $\delta^{18}O$ (Fig. 6A) reflects a prolonged interval of convection north of Iceland. Indeed, this interval coincides with an increase in coccoliths associated with the North Atlantic Drift in core 330 from the inner shelf [44] (Fig. 1). There is no systematic correlation between the NAO winter index [64] and the timing of low wind stress curl regimes over the Greenland Sea north of Iceland. However, there is a strong negative correlation between the wind curl stress and the thickness of freshwater in spring over the Iceland Sea, and over the last 40 yr negative NAO years are associated with very low wind stress curl values across the Iceland Sea [63].

The PC1 time series consists of a record that is unlikely to have arisen from random climate noise (Figs. 4 and 5). Statistically significant relationships, moreover, are established between the inferred oscillatory variations in subsurface ocean circulation changes in the North Atlantic and independently documented variations in solar variability on multidecadal through multi-millennial timescales. Previous evidence for significant multidecadal variability in the North Atlantic, and possible relationships to solar forcing, has been based on analyses of annually resolved surface proxy indicators, such as tree-rings, ice cores, corals, and historical records (e.g. [58] and references therein). We have presented here a new multidecadal marine data set from the northern North Atlantic. Analysis of these data verifies a close apparent longer-term relationship between multidecadal North Atlantic oceanographic variability and solar forcing.

The findings presented here also complement other previous evidence for significant relationships between Holocene solar and surface oceanographic variations (e.g. Fig. 6) at longer timescales, such as inferred millennial-scale changes in drift ice [65] by establishing evidence of millennial-scale oceanographic variations within the subsurface structure of the ocean, and by clarifying the significant timescales of variability based on considerably better frequency control. Bond et al. (see e.g. their supplementary figure 3 [65]) found broad, moderately (90%) significant spectral peaks in the frequency ranges 0.4–1.4 cycle/kyr (700–2500 years), 1.9–2.5 cycles/kyr (400–530 year) and 4.3–4.7 cycles/kyr (210–230 years). Our higher resolution analysis verifies such broad peaks, but shows them often to be composed of groups of more statistically significant, but more narrowband variability. The fine structure of these narrowband signals corresponds with the fine structure evident in long proxies for solar variability.

The observations presented here should consti-

tute a useful extended target for dynamical modeling approaches [55,59] to understanding forced patterns of climate variability during the Holocene.

Acknowledgements

References

[1] S.-A. Malmberg, Hydrographic Changes in the Waters Between Iceland and Jan Mayen in the Last Decade, Jokull 19 (Symposium on Drift Ice and Climate), 1969, pp. 30–43.

[2] S.-A. Malmberg, The water masses between Iceland and Greenland, J. Mar. Res. Inst. 9 (1985) 127–140.

[3] R.R. Dickson, H.H. Lamb, S.-A. Malmberg, J.M. Colebrook, Climatic reversal in northern North Atlantic, Nature 256 (1975) 479–482.

[4] J. Olafsson, Connections between oceanic conditions off N-Iceland, Lake Myvatn temperature, regional wind direction variability and the North Atlantic Oscillation, Rit Fiskid. 16 (1999) 41–57.

[5] H.H. Lamb, Climatic variations and changes in the wind and ocean circulation: The Little Ice Age in the Northeast Atlantic, Quat. Res. 11 (1979) 1–20.

[6] S. Thorarinsson, Oscillations of Iceland glaciers during the last 250 years, Geogr. Ann. 25 (1953) 1–54.

[7] G. Helgadottir, Paleoclimate (0 to >14 ka) of W. and NW Iceland: An Iceland/USA Contribution to P.A.L.E., Cruise Report B9-97, Marine Research Institute of Iceland, Reykjavik, 1997.

[8] J.T. Andrews, J. Hardarddottir, G. Helgadottir, A.E. Jennings, A. Geirsdottir, A.E. Sveinbjornsdottir, S. Schoolfield, G.B. Kristjansdottir, L.M. Smith, K. Thors, J.P.M. Syvitski, The N and W Iceland Shelf: Insights into Last Glacial Maximum Ice Extent and Deglaciation based on Acoustic Stratigraphy and Basal Radiocarbon AMS dates, Quat. Sci. Rev. 19 (2000) 619–631.

[9] U. Stefansson, North Icelandic Waters, Rit Fiskideildar III. Bind, Vol. 3, 1962.

[10] J.T. Andrews, G. Helgadottir, Late Quaternary ice cap extent and deglaciation of Hunafloaall, NorthWest Iceland: Evidence from marine cores, Arctic, Antarctic, and Alpine Research, 2003.

[11] J. Eiriksson, K.L. Knudsen, H. Haflidason, P. Henriksen, Late-glacial and Holocene paleoceanography of the North Iceland Shelf, J. Quat. Sci. 15 (2000) 23–42.

[12] T.S. Hopkins, The GIN Sea – A synthesis of its physical oceanography and literature review 1972–1985, Earth Sci. Rev. 30 (1991) 175–318.

[13] J. Rumohr, F. Blaume, H. Erlenkeuser, H. Fohrmann, F.-J. Hollender, J. Mienert, C. Schafer-Neth, Records and processes of near-bottom sediment transport along the Norwegian–Greenland Sea margins during Holocene and Late Weischelian (Termination I) time, in: P. Schafer, W. Ritzrau, M. Schulter, J. Thiede (Eds.), The Northern North Atlantic: A Changing Environment, Springer-Verlag, Berlin, 2001, pp. 155–178.

[14] K.H. Michels, Inferring maximum geostrophic current velocities in the Norwegian–Greenland Sea from settling-velocity measurements of sediment surface samples: Method, application, and results, J. Sediment. Res. 70 (2000) 1036–1050.

[15] S. Jónsson, J. Briem, Flow of Atlantic Water west of Iceland and onto the north Iceland shelf, in press.

[16] J.T. Andrews, R. Kihl, G.B. Kristjánsdóttir, L.M. Smith, G. Helgadóttir, Á. Geirsdóttir, A.E. Jennings, Holocene sediment properties of the East Greenland and Iceland continental shelves bordering Denmark Strait (64°–68°N), North Atlantic, Sedimentology 49 (2002) 5–24.

[17] R.J. Weeks, C. Laj, L. Endignoux, M.D. Fuller, A.P. Roberts, R. Manganne, E. Blanchard, W. Goree, Improvements in long core measurement techniques: applications in paleomagnetism and paleoceanography, Geophys. J. Int. 114 (1993) 651–662.

[18] K. Verosub, Paleomagnetic dating, in: J.S. Noller, J.M. Sowers, W.R. Lettis (Eds.), Quaternary Geochronology. Methods and Applications, America Geophysical Union, Washington, DC, 1999, pp. 339–356.

[19] L. Tauxe, Sedimentary records of relative paleointensity of the geomagnetic field: Theory and practice, Rev. Geophys. 31 (1993) 319–354.

[20] D. Paillard, L. Labeyrie, P. Yiou, Macintosh Program Performs Time-Series Analysis, EOS 77 (1996) 379.

[21] R. Thompson, F. Oldfield, Environmental Magnetism, Allen and Unwin, Winchester, MA, 1986, 227 pp.

[22] J. Walden, F. Oldfield, J. Smith, Environmental magnetism. A practical guide, in: Technical Guide No. 6, Quaternary Research Association, London, 1999, p. 243.

[23] B.A. Maher, R. Thompson, M.W. Hounslow, Introduction, in: B.A. Maher, R. Thompson (Eds.), Quaternary Climates, Environments, and Magnetism, Cambridge University Press, Cambridge, 1999, pp. 1–48.

[24] M. Stuiver, P.J. Reimer, E. Bard, J.W. Beck, K.A. Hughen, B. Kromer, F.G. McCormack, J. vdPlicht, M. Spurk, INTCAL98 Radiocarbon age calibration 24,000–0 cal BP, Radiocarbon 40 (1998) 1041–1083.

[25] G.B. Kristjansdottir, Holocene Hekla tephras: A stratigraphic tool for estimating changes in reservoir age of seawater, Core MD99-2269, NW-Iceland shelf, in: 31nd Arctic Workshop, INSTAAR, University of Colorado, Boulder, CO, 2002, pp. 103–104.

[26] H. Haflidason, J. Eiriksson, S. VanKreveld, The tephrachronology of Iceland and the North Atlantic region during the Middle and Late Quaternary: a review, J. Quat. Sci. 15 (2000) 3–22.

[27] J.T. Andrews, A. Geirsdottir, J. Hardardottir, S. Principato, K. Gronvold, G.B. Krisjansdottir, G. Helgadottir, J. Drexler, A. Sveinbjornsdottir, Distribution, sediment magnetism, and geochemistry of the Saksunarvatn (10.18 ± cal ka) tephra in marine, lake, and terrestrial sediments, NW Iceland, J. Quat. Sci. 17 (2002) 731–745.

[28] K. Gronvold, N. Oskarsson, S.J. Johnsen, H.B. Clausen, C.U. Hammer, G. Bond, E. Bard, Ash layers from Iceland in the Greenland GRIP ice core correlated with oceanic and land sediments, Earth Planet. Sci. Lett. 135 (1995) 149–155.

[29] H.H. Birks, S. Gulliksen, H. Haflidason, J. Mangerud, G. Possnert, New Radiocarbon Dates for the Vedde Ash and the Saksunarvatn Ash from Western Norway, Quat. Res. 45 (1996) 119–127.

[30] M. Wastl, J. Stotter, C. Caseldine, Tephrochronology–A tool for correlating records of Holocene environmental and climatic change in the North Atlantic region, Geol. Soc. Am. Abstr. 31 (1999) A315.

[31] M. Schulz, K. Stattegger, Spectrum: spectral analysis of unevenly spaced paleoclimatic time series, Comput. Geosci. 23 (1997) 929–945.

[32] D.M. Anderson, Attenuation of millennial-scale events by bioturbation in marine sediments, Paleoceanography 16 (2001) 352–357.

[33] J.T. Andrews, J. Hardardottir, G.B. Kristjansdottir, K. Gronvald, J. Stoner, A very high resolution Holocene sediment record (5 yr/cm) from Húnflóaáll, N Iceland margin: Century to millennial-scale variability since the Vedde tephra, The Holocene, in press.

[34] J.C. Davis, Statistics and data analysis in Geology, John Wiley and Sons, New York, 1986, 646 pp.

[35] F. Heider, J.M. Bock, I. Hendy, J.P. Kennett, J. Matzka, J. Schneider, Latest Quaternary rock magnetic record of climatic and oceanic change, Tanner Basin, California borderland, Geol. Soc. Am. Bull. 113 (2001) 346–359.

[36] I.N. McCave, B. Manighetti, N.A.S. Beveridge, Circula-

tion in the glacial North Atlantic inferred from grain-size measurements, Nature 374 (1995) 149–152.

[37] I.N. McCave, B. Manighetti, S.G. Robinson, Sortable silt and fine sediment size/composition slicing: Parameters for palaeocurrent speed and palaeoceanography, Paleoceanography 10 (1995) 593–610.

[38] G.G. Bianchi, I.N. McCave, Holocene periodicity in North Atlantic climate and deep-ocean flow south of Iceland, Nature 397 (1999) 515–517.

[39] J.T. Andrews, C. Caseldine, N.J. Weiner, J. Hatton, Late Quaternary (∼4 ka) Marine and Terrestrial Environmental Change in Reykjarfjördur, N. Iceland: Climate and/or Settlement?, J. Quat. Sci. 16 (2001) 133–144.

[40] J.T. Andrews, G. Helgadottir, A. Geirsdottir, A.E. Jennings, Multicentury-scale records of carbonate (hydrographic?) variability on the N. Iceland margin over the last 5000 yrs, Quat. Res. 56 (2001) 199–204.

[41] T. Thordardottir, Primary production in North Icelandic Waters in relation to Recent Climatic Change, Polar Oceans: Proceedings of the Oceanographic Congress, 1977, pp. 655–665.

[42] T. Thordardottir, Primary Production North of Iceland in relation to Water Masses in May–June 1970–1980, Council for the Exploration of the Sea, C.M. 1984/L20, 1984, pp. 1–17.

[43] G.B. Kristjansdottir, J.T. Andrews, A.E. Jennings, A. Geirsdottir, S. Principato, Preliminary results for three MD99 marine sedimentary cores on the W and NW Iceland shelf, in: Changes in Climate and Environment at High Latitudes, Tromso, 2001, p. 62.

[44] J.T. Andrews, J. Giradeau, Multi-proxy records showing significant Holocene environmental variability: the inner N Iceland Shelf (Hunafloi), Quat. Sci. Rev. 22 (2003) 175–194.

[45] I.S. Castaneda, Holocene paleoceanographic and climatic variations of the inner North Iceland continental shelf, Reykjarfjorddur area, M.Sc. thesis, University of Colorado, Boulder, CO, 2001.

[46] L.M. Smith, Holocene paleoenvironmental reconstruction of the continental shelves adjacent to the Denmark Strait, Ph.D. thesis, University of Colorado, Boulder, CO, 2001.

[47] W.H. Berger, J. Pätzold, G. Wefer, A case for climate cycles: Orbit, sun and moon, in: G. Wefer, W.H. Berger, K.-E. Behre, E. Jansen (Eds.), Climate Development and History of the North Atlantic Realm, Springer-Verlag, Berlin, 2002, pp. 101–123.

[48] R.B. Alley, S. Anandakrishnan, P. Jung, Stochastic resonance in the North Atlantic, Paleoceanography 16 (2001) 190–198.

[49] G. Bond, W. Showers, M. Cheseby, R. Lotti, P. Almasi, P. deMenocal, P. Priore, H. Cullen, I. Hajdas, G. Bonani, A pervasive millennial-scale cycle in North Atlantic Holocene and glacial climates, Science 278 (1997) 1257–1266.

[50] R.G. Douglas, D. Gorsline, A. Grippo, I. Granados, O. Yajimovich-Gonzalez, Holocene ocean-climate variations in Alfonso Basin, Gulf of California, Mexico, in: J. West, J.B. Bullaloe (Eds.), 18th Annual Pacific Climate Work-

shop, Interagency Ecological Program for San Francisco Estuary, Technical Report 69, 2001, pp. 7–20.

[51] M.E. Mann, J.M. Lees, Robust estimation of background noise and signal detection in climatic time series, Clim. Change 33 (1996) 409–445.

[52] P.U. Clark, S.J. Marshall, G.K.C. Clarke, S.W. Hostetley, J.M. Licciardi, J.T. Teller, Freshwater forcing of abrupt climate change during the last glaciation, Science 293 (2001) 283–287.

[53] D.J. Thompson, Time series analysis of Holocene climate data, Philos. Trans. R. Soc. London 330 (1990) 601–616.

[54] P.E. Damon, C.J. Eastoe, M.K. Hughes, R.M. Kalin, A. Long, A.N. Peristykh, Secular variation of delta 14C during the Medieval solar maximum: A progress report, Radiocarbon 40 (1998) 343–350.

[55] D.T. Shindell, G.A. Schmidt, M.E. Mann, D. Rind, A. Waple, Solar forcing of regional climate change during the Maunder Minimum, Science 294 (2001) 2149.

[56] M. Ram, M.R. Stolz, Possible solar influence on the dust profile of the GISP2 ice core from Central Greenland, Geophys. Res. Lett. 26 (1999) 1043–1046.

[57] S.R. O'Brian, P.A. Mayewski, L.D. Meeker, D.A. Meese, M.S. Twickler, S.I. Whitlow, Complexity of Holocene climate as reconstructed from a Greenland ice core, Science 270 (1995) 1962–1964.

[58] T.L. Delworth, M.E. Mann, Observed and simulated multidecadal variability in the Northern Hemisphere, Climate Dyn. 16 (2000) 661–676.

[59] U. Cubasch, R. Voss, G.C. Hegerl, J. Waskewitz, T.J. Crowley, Simulation of the influence of solar radiation variations on the global climate with an ocean-atmosphere general circulation model, Climate Dyn. 13 (1997) 757–767.

[60] P.E. Delworth, K.W. Dixon, Implications of the recent trend in the Arctic/North Atlantic Oscillation for the North Atlantic thermohaline circulation, J. Climate 13 (2001) 3721–3727.

[61] T.L. Delworth, S. Manabe, R.J. Stouffer, Multidecadal climate variability in the Greenland Sea and surrounding regions: a coupled model simulation, Geophys. Res. Lett. 24 (1997) 257–260.

[62] C. Lacasse, Influence of climatic variability on the atmospheric transport of Icelandic tephra in the subpolar North Atlantic, Glob. Planet. Change 29 (2001) 31–56.

[63] S.-A. Malmberg, S. Jonsson, Timing of deep convection in the Greenland and Iceland Seas, J. Mar. Sci. 54 (1997) 300–309.

[64] J.W. Hurrell, Y. Kushnir, M. Visbeck, The North Atlantic Oscillation, Science 291 (2001) 603–604.

[65] G. Bond, B. Kromer, J. Beer, R. Muscheler, M.N. Evans, W. Showers, S. Hoffman, R. Lotti-Bond, I. Hajdas, G. Bonani, Persistent solar influence on North Atlantic climate during the Holocene, Science 294 (2001) 2130.

[66] T.M. Rittenour, J. Brigham-Grette, M.E. Mann, El Nino-like climate teleconnections in New England during the Late Pleistocene, Science 288 (2000) 1039–1042.